

Effect of Semiconductor on Sensitivity of a Graphene-Based Surface Plasmon Resonance Biosensor

Goutam Mohanty¹ · Jamil Akhtar² · Bijay Kumar Sahoo¹

Received: 5 May 2015 / Accepted: 26 July 2015 / Published online: 7 August 2015
© Springer Science+Business Media New York 2015

Abstract In this theoretical study, the effect of semiconductor on sensitivity of a graphene-based surface plasmon resonance (SPR) biosensor has been presented. Different semiconductors such as silicon (Si), germanium (Ge) and wurtzite III-V nitrides (AlN, GaN and InN) have been placed in between active silver (Ag) metal and graphene layer. Our simulation result shows that addition of semiconductor layer enhances the sensitivity by a factor of 3.76, 2.19, 3.82, 3.94 and 4.17 respectively for Si, Ge, InN, GaN and AlN. Also, we have examined the field enhancement factor due to above semiconductors and found maximum field intensity enhancement for the case of AlN. The analysis shows that best performance is achieved for red He-Ne laser light when optimized thicknesses of silver, AlN and graphene layer are 55, 14 and 0.34 nm (monolayer of graphene), respectively. More specifically, AlN would be a better choice for biosensing application in SPR biosensor.

Keywords SPR biosensor · Semiconductor · Sensitivity · Field enhancement

Introduction

Surface plasmon resonance (SPR) is a simple and direct optical sensing technique that is used to investigate refractive index change that occurs in the vicinity of a thin noble metal film.

The potential use of SPR for gas molecule detection and biosensing was first demonstrated by Nylander and co-workers [1, 2]. Later on, SPR biosensing has received a great attention from the scientific community. The advantage of employing SPR in biosensing lies in its capability of monitoring binding interactions without the need for labelling and fluorescence of the biomolecules. In addition, this technique has shown great potential in the real-time determination of the concentration, kinetic constant and binding specificity of individual biomolecular interactions. Antibody–antigen interactions [3–5], peptide–protein interactions [6] and DNA hybridization [7] can all be analysed.

In order to monitor surface interactions in a sensitive and stable manner with SPR biosensors, one should give attention in three vital areas. It is necessary that the SPR sensor is highly sensitive to binding interactions within the sensing region, the reflectivity dip has a narrow full-width-half-maximum (FWHM) and the metal film is highly stable even under extreme environmental conditions [8]. Due to different optical and chemical properties of individual metal films, the realization of all three conditions is not possible simultaneously with a conventional SPR sensor. The choice of metal used is critical since the metal must exhibit free electron behaviour as described by the free electron model. To be useful for SPR, a metal must have conduction band electrons capable of resonating with light at a suitable wavelength. Silver [9] and gold [10] are two such metallic elements that satisfy this condition, and they are more popularly used in research and commercial applications because of their sensitivity and stability, respectively. Instead of the above-mentioned metals, other metals like copper, aluminium and palladium may be used over the prism surface.

The drawback with gold is that it is a poor adsorbent of biomolecules, thereby limiting the sensitivity of the biosensor. Generally, a silver film with a sharp SPR curve may yield a higher imaging sensitivity than a gold film. However, the sensitivity of the silver-based SPR biosensor has a potential

✉ Goutam Mohanty
gmohanty.phd2012.phy@nitrr.ac.in

¹ Department of Physics, N.I.T Raipur, G. E. Road, Raipur, CG 492010, India

² Sensor and Nanotechnology Group, CSIR-CEERI, Pilani, Raj 333031, India

limitation, because silver is highly susceptible to oxidation. While the use of a thin gold film might be a better choice in terms of stability and reliability, silver would be a promising candidate for sensitive SPR imaging detection if silver surfaces can be made chemically inert. To enhance the sensitivity of conventional SPR biosensor, researchers have been used graphene on the surface of metals [11]. It possesses very fascinating optical, mechanical and electrical properties which have attracted many researchers and scientists all over the world. The advantage of graphene on gold is that it helps to adsorb more and more ring-type biomolecules [12], and in case of silver, the advantage is that it prevents the oxidation of silver layer [13–15]. Recently, Verma et al. [16] have demonstrated theoretically that the addition of silicon (Si) layer between gold and graphene enhances the sensitivity of SPR biosensor twice the value reported in the literature. The reason of enhancement of the change in resonance angle or the sensitivity is the high refractive index of the silicon layer which increases the field intensity at the interface; hence, the field penetrates strongly into the analyte. It is to be pointed out that a number of groups have reported both experimentally and theoretically the effects due to elevated temperatures on the surface plasmon at a metal–semiconductor interface. The results show that the strength of the surface plasmon (SP) at the junction will decrease as temperature increases. The SPR curve is shifted and broadened at high temperatures because properties of the metal layer and prism depend on temperature [17]. The resonance position shifts to a smaller value, and the sensitivity becomes lower with increasing temperature. The properties of semiconductor layer are also very sensitive to temperature rise.

Past study reports that the temperature effect on the metal film and the prism provides an opposite shift to the resonant position of the SPR curve. As semiconductor is a part of our proposed model, the temperature effects on semiconductor layer need to be minimized for achieving maximum sensitivity. Thus, a semiconductor material that possesses high refractive index and high temperature resistance is required to be investigated. In this regard, wurtzite III-V nitrides are the most promising candidates. They possess a number of superior properties in addition to high refractive index and high temperature resistance. They have already established themselves as the basic material next to silicon/germanium in fabrication of thin films optoelectronics devices. They are nontoxic and biofriendly and can be easily attached with graphene due to hexagonal unit cell structures. Recently, Makowski et al. [18] have demonstrated GaN can be used for the detection of hexylamine and peptide. To the best of the authors' knowledge, the potential of nitrides for active Ag metal in the SPR sensor keeping in mind high sensitivity at ambient temperatures and high field enhancement at analyte region has not been analysed. In the present study, we have theoretically addressed the effect of wurtzite III-V nitride as well as silicon and germanium on the sensitivity of a graphene-based SPR biosensor.

Theory and Principle

Surface plasmon polariton (SPP) wave is an electromagnetic wave propagating at the interface between a metal and a dielectric, evanescently confined in the perpendicular direction. Here, the dielectric layer is a sensing medium that may be water, blood, serum and urine, etc. When p -polarized light incident on the noble metal surface at resonance angle (θ_{res}) through another dielectric medium (here, it is a glass prism), SPW will be produced at the metal–dielectric interface and this information can be observed optically in terms of total internal reflection. This concept was first introduced experimentally by Otto [19] and later by Kretschmann [20] which is known as prism coupler method. At resonance condition, wave vector of incident p -polarized light and surface plasmon must be equal which can be written as:

$$\frac{2\pi}{\lambda} n_p \sin \theta_{\text{res}} = \frac{\omega}{c} \sqrt{\frac{\epsilon_m \epsilon_d}{\epsilon_m + \epsilon_d}} \quad (1)$$

where λ is the wavelength of red He-Ne laser light, n_p is the refractive index of prism, θ_{res} is the resonance angle, ω is the angular frequency of plasmon, ϵ_m is the dielectric constant of the metal and ϵ_d is the dielectric constant of the dielectric layer.

Computational Methodology In the proposed model, we have taken N -layer structure for computing the reflectance co-efficient by using transfer matrix method (TMM) [21–23], where $N=6$. Here, the layers are placed according to the following manner, i.e. prism: silver: semiconductor: graphene: biomolecular layer: sample, as shown in Fig. 1. The target biomolecules (such as hexagonal/ring type) are present in the sample solution which can be attracted by graphene layer due to the adsorption nature of graphene layer; hence, additional layer, called biomolecular layer (or) binding layer, is induced on the surface of graphene. The biomolecular layer has somewhat higher refractive index than the sensing medium, and this change in refractive index will modify the

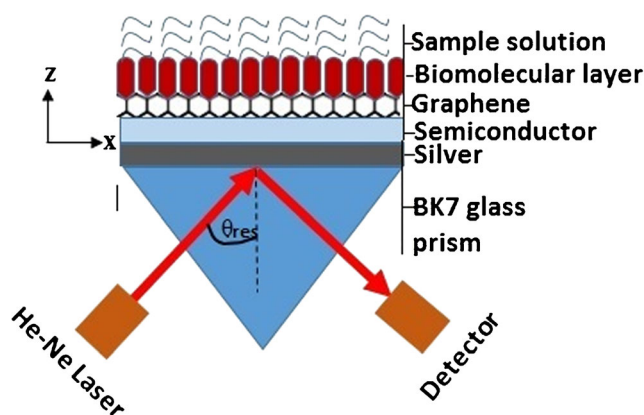


Fig. 1 Schematic diagram of SPR biosensor

Table 1 Optical properties of materials at 632.8 nm wavelength of light

Material	Refractive index (n)	Extinction co-efficient (k)	References
BK7 glass prism	1.5151	0	[25]
Silver (Ag)	0.05625	4.2760	[26]
Graphene	3	1.149106	[27]
Silicon (Si)	3.8827	0.019626	[28]
Germanium (Ge)	5.4717	0.81627	[28]
Aluminium nitride (AlN)	2.1496	0	[29]
Gallium Nitride (GaN)	2.3848	0	[30]
Indium nitride (InN)	2.9	0	[31]
Water	1.3317	0	[32]

propagation constant of plasma wave. As a result, the propagation constant can be optically measured in terms of reflection co-efficient. The reflectance co-efficient of N -layer system for p -polarized light is [12, 21, 24]:

$$R = \left| \frac{(M_{11} + M_{12}q_N)q_1 - (M_{21} + M_{22}q_N)}{(M_{11} + M_{12}q_N)q_1 + (M_{21} + M_{22}q_N)} \right|^2 \tag{2}$$

where $M_{ij} = \left(\prod_{k=2}^{N-1} M_k \right)_{ij}; i, j = 1, 2;$

and $M_k = \begin{pmatrix} \cos\beta_k & -i\sin\frac{\beta_k}{q_k} \\ -iq_k\sin\beta_k & \cos\beta_k \end{pmatrix}; q_k = \frac{(\epsilon_k - n_1^2 \sin^2\theta)^{1/2}}{\epsilon_k}; \beta_k = d_k \left(\frac{2\pi}{\lambda} \right) (\epsilon_k - n_1^2 \sin^2\theta)^{1/2}$

When the reflectance co-efficient (R) reaches its lowest value, the intensity of the electromagnetic field reaches its maximum at the metal surface. It is known that electric field is not continuous across the metal–dielectric interface, but magnetic field is continuous across all boundaries for p -polarized light. Hence, the magnetic field intensity is first

calculated using Eqs. (3a), and then, electric field intensity can be calculated using Eqs. (3b).

The electromagnetic (EM) fields are [21]:

$$H_{\perp} = \frac{2 \times q_1}{(M_{11} + M_{12}q_N)q_1 + (M_{21} + M_{22}q_N)} \tag{3a}$$

$$E_{\parallel} = \frac{\mu_N n_1}{\mu_1 n_N} H_{\perp} \tag{3b}$$

The refractive index of different materials used for computation of important parameters such as reflectance co-efficient, FWHM and field intensity is mentioned in the Table 1. Assuming that biomolecular reactions produce a change in refractive index 1.462 of the biomolecular layer and do not induce a change in thickness, here, the thickness of biomolecular layer is taken 10 nm for the computation. The performance of the SPR biosensor has been evaluated in terms of three aspects, i.e. *first*, shift in resonance angle for a given change in the sensing layer refractive index should be maximized. Mathematically,

$$\text{Sensitivity}(S) = \frac{\Delta\theta}{\Delta n} \Rightarrow S \propto \Delta\theta \tag{4}$$

Second, the FWHM corresponding to the SPR curves should be minimized so that the error in determining the resonance angle is minimal. Mathematically, Sensitivity (S) $\propto \frac{1}{\text{FWHM}}$

Third, the stronger evanescent field implies a larger sensing region for monitoring cell interactions; hence, higher sensitivity can be achieved.

Results and Discussion

In the proposed model, the active metal has been chosen as silver (Ag). The structure of the sensor such as silver: semiconductor: graphene: binding layer: samples is arranged layer

Fig. 2 Change in resonance angle due to the effect of Si w.r.t graphene layers

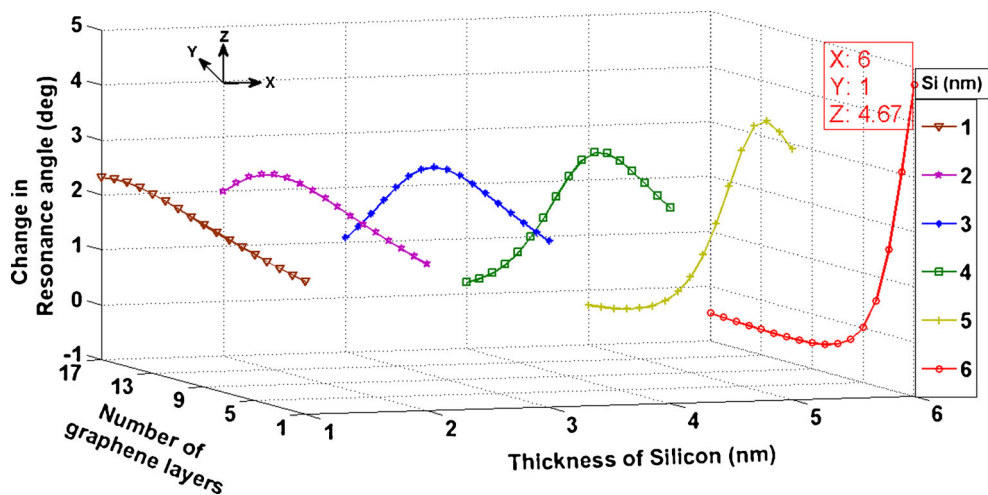
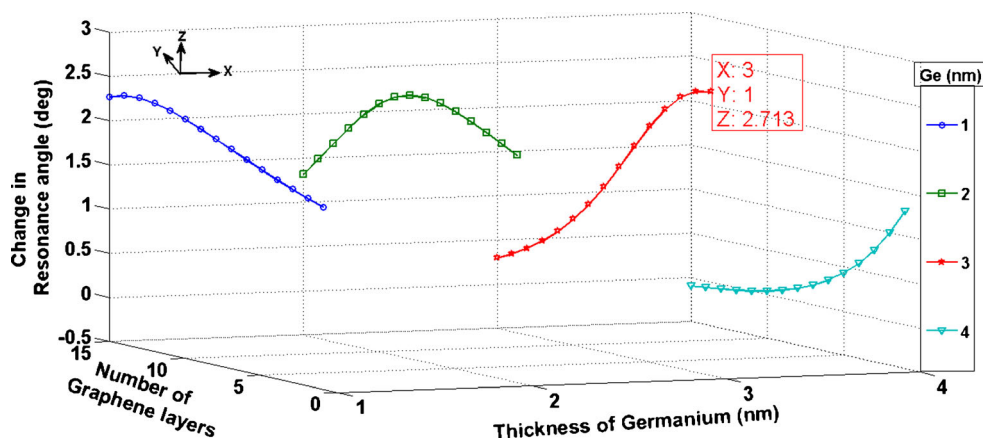


Fig. 3 Change in resonance angle due to the effect of Ge w.r.t graphene layers



by layer and is positioned on the surface of the BK7 glass prism. We have examined the influence of semiconductors such as Si, Ge, AlN, GaN and InN on the sensitivity of the sensor. Using TMM method, we have computed attenuated total reflection co-efficient (R), full-width-half-maxima (FWHM) and field intensity for a p -polarized red He-Ne laser light. A MATLAB-based simulation is performed for the computation of the above-mentioned parameters. First, the thickness of metal (here, it is Ag) layer has been optimized for achieving minimum reflectance without using graphene and semiconductor layers. The optimized thickness has been found as 55 nm. When graphene layers are deposited over metal surface, target analyst present on sample will be adsorbed on the graphene surface. Due to this adsorption, a binding layer/biomolecular layer is formed on the graphene surface. Now, the resonance angle will shift after the formation of binding layer. This happens due to change in refractive index of binding layer after its formation. But when semiconductor layers are placed between Ag and graphene, it has been observed that the resonance angle further shifts. The shift is comparatively higher in the latter case. To check the performance of the sensor, we have observed the resonance angle (θ) obtained before and after the formation of binding layer over

the graphene layer. As the sensitivity of SPR sensor is directly proportional to the change in resonance angle ($\Delta\theta$) as shown in Eq. (4), the maximum change in resonance angle ($\Delta\theta_{\max}$) would imply higher sensitivity. In this work, we have optimized the thickness of graphene and semiconductor layers for achieving $\Delta\theta_{\max}$.

First, we have examined the effect of silicon layers on the sensitivity of the proposed sensor. We have optimized the thickness of the silicon with respect to number of graphene layers for maximum sensitivity. The change in resonance angle ($\Delta\theta$) as a function of graphene layer and Si-layer has been shown in the Fig. 2. From the figure, it can be observed that the $\Delta\theta$ becomes maximum when number of graphene layer is one and thickness of Si-layer is 6 nm. The maximum change in resonance angle ($\Delta\theta_{\max}$) is found as 4.67° in this case. For the above values of graphene and semiconductor layer, FWHM has also been computed and found as 7.26° . In addition, it is to be noted that the $\Delta\theta$ for optimal thickness of Ag and for a single layer of graphene has also been computed in the absence of Si-layer and found as 1.241° . Thus, one can predict that addition of Si-layer improves the sensitivity by a factor of 3.76. Similar procedure is applied to all other semiconductors.

Fig. 4 Change in resonance angle due to the effect of InN w.r.t graphene layers

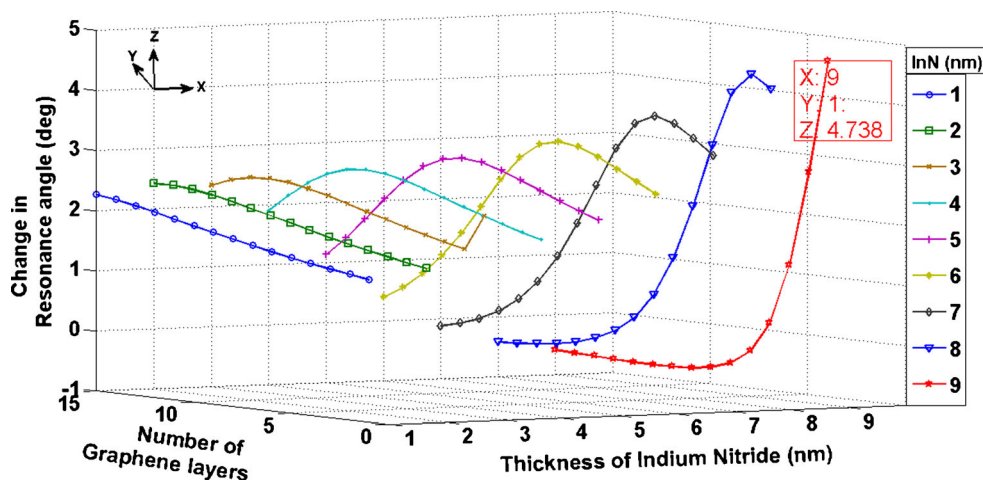
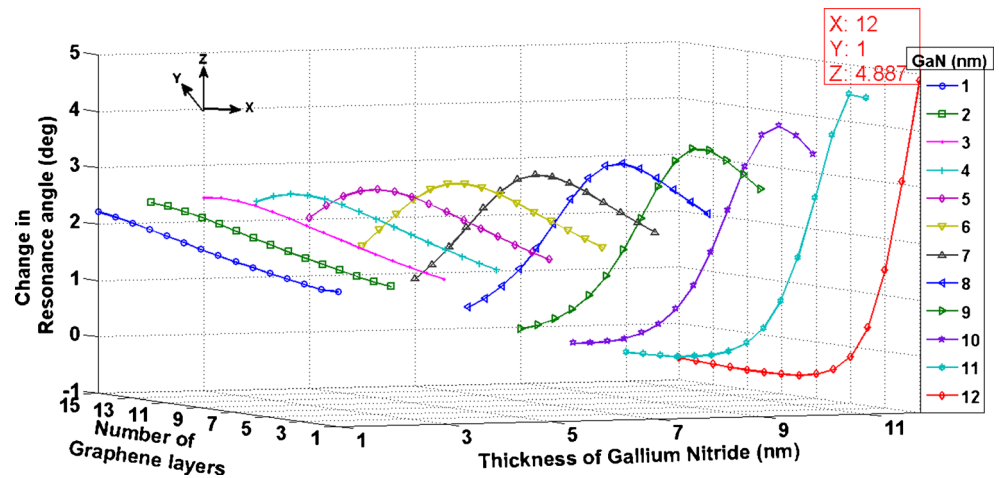


Fig. 5 Change in resonance angle due to the effect of GaN w.r.t graphene layers



In the second step, we have examined the effect of germanium (Ge) semiconductor on the sensitivity of the proposed sensor. Figure 3 shows the change in resonance angle ($\Delta\theta$) as a function of graphene and Ge thickness. From Fig. 3, it can be observed that for a single graphene layer, maximum change occurs in the resonance angle. This maximum change becomes 2.713 and 1.241° for with and without Ge-layer. Thus, one can find that addition of Ge-layer between Ag and graphene enhances the sensitivity by a factor of 2.19. Also, FWHM has been computed for the optimal values of Ge-layer and found as 10.72°. It is to be noted that this FWHM is wider than the case of Si. Thus, one can predict that Si-based SPR sensor will have high sensitivity and high precision than Ge-based sensor.

Now, we are interested to examine the effect of wurtzite nitrides like InN, GaN and AlN. Figure 4 shows the change in resonance angle ($\Delta\theta$) as a function of graphene and InN thickness. From Fig. 4, it can be observed that for a single graphene layer, maximum change occurs in the resonance angle similar to Ge-based sensor. This maximum change becomes 4.738 and 1.241° for with and without InN layers. Thus, one can find that addition of InN layer between Ag and graphene enhances the sensitivity by a factor of 3.82. Also, FWHM has

been computed for optimal thickness of InN and found as 6.80°. It is to be noted that this FWHM is narrower than the case of Si and Ge.

figure 5 shows the change in resonance angle ($\Delta\theta$) as a function of graphene and GaN thickness. From Fig. 5, it can be observed that for a single graphene layer, maximum change occurs in the resonance angle. This maximum change becomes 4.887 and 1.241° for with and without GaN layers. Thus, one can find that addition of GaN layer between Ag and graphene enhances the sensitivity by a factor of 3.94. Also, FWHM has been computed for the optimal thickness of GaN and found as 6.54°. It is to be noted that this FWHM is narrower than the case of Si, Ge and InN.

figure 6 shows the change in resonance angle ($\Delta\theta$) as a function of graphene and AlN thickness. From Fig. 6, it can be observed that for a single graphene layer, maximum change occurs in the resonance angle. This maximum change becomes 5.175 and 1.241° for with and without AlN layers. Thus, one can find that addition of AlN layer between Ag and graphene enhances the sensitivity by a factor of 4.17. Also, FWHM has been computed for the optimal thickness of AlN and found as 6.16°. It is to be noted that this FWHM is narrower than the case of Si, Ge, InN and GaN.

Fig. 6 Change in resonance angle due to the effect of AlN w.r.t graphene layers

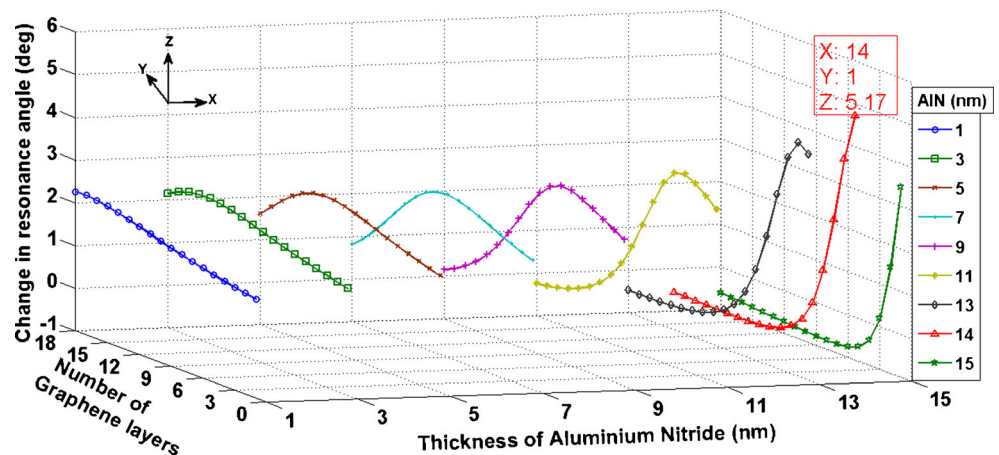


Table 2 Change in resonance angle and FWHM for various semiconductors

Semiconductor	Thickness of semiconductor (nm)	Thickness of Ag (nm)	No. of graphene layer	Resonance angle (θ_1) without binding layer (deg.)	Resonance angle (θ_2) with binding layer (deg.)	Change in resonance angle, $\Delta\theta$ (deg.)	FWHM (deg.)	Increase in $\Delta\theta$
Si	0	55	1	67.73	68.971	1.241	–	3.76 times
Si	6	55	1	81.134	85.804	4.67	7.26	
Ge	0	55	1	67.73	68.971	1.241	–	2.19 times
Ge	3	55	1	75.933	78.646	2.713	10.72	
InN	0	55	1	67.73	68.971	1.241	–	3.82 times
InN	9	55	1	81.469	86.207	4.738	6.80	
GaN	0	55	1	67.73	68.971	1.241	–	3.94 times
GaN	12	55	1	81.394	86.281	4.887	6.54	
AlN	0	55	1	67.73	68.971	1.241	–	4.17 times
AlN	14	55	1	80.55	85.725	5.175	6.16	

Above findings are summarized in the Table 2. It shows the change in resonance angle ($\Delta\theta$) and FWHM for various semiconductor layers with optimal values of Ag and graphene with and without binding layers. The highest change in resonance angle and narrow FWHM is clearly observed for AlN. This suggests that AlN can be a superior choice than the other considered semiconductors for active Ag metal.

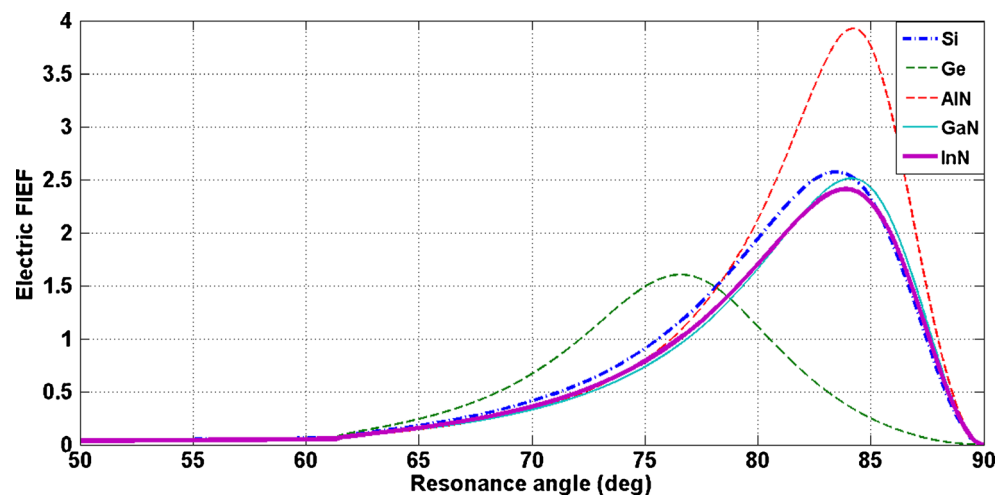
In addition, we have studied how field intensity at the sensor surface affects by placing various semiconductors in between active Ag metal and graphene layer. The performance of SPR sensor depends on the field distribution of surface plasmons at metal–dielectric interface. It is well known that the electromagnetic (EM) field of SPs at the metal–sensing layer interface decays exponentially within only a fraction of a wavelength which is termed as evanescent field. The associated EM field distribution of SPs is important for SPR sensors because the interaction of evanescent field with molecules in the sensing region is vital. If the field distribution is enhanced, then, more biomolecular interaction takes place; hence, sensitivity will be enhanced. One can achieve this by increasing the field's peak height at metal–sensing layer interface. In order to understand the field peak height, we carried

out the study of electric field intensity enhancement factor (EFIEF) at interface for each semiconductor.

Mathematically, Eq. (3b) can be written as [21, 33],

$$\left| \frac{E_{\parallel}(N/N-1)}{E_{\parallel}(1/2)} \right|^2 = \frac{\epsilon_1}{\epsilon_N} \left| \frac{H_{\perp}(N/N-1)}{H_{\perp}(1/2)} \right|^2 \quad (5)$$

figure 7 shows the variation of electric FIEF for various semiconductor-based SPR sensors with optimized thickness of metal and graphene layers. It is known that the propagation of electromagnetic wave in a material with complex refractive index is attenuated as a function of distance. Here, imaginary part (extinction co-efficient, k) of a complex refractive index represents an attenuation of the wave. Our simulation result shows that Si has higher FIEF than the Ge because the extinction co-efficient of Si (0.019626) is smaller than the Ge (0.81627). This indicates that maximum EFIEF is achieved for semiconductors having smaller k -value. It is to be pointed out that III-V nitrides have zero extinction co-efficient for 632.8 nm wavelength of light. We have simulated EFIEF for III-V nitrides (AlN, GaN and InN). Our simulation result shows that the highest EFIEF is achieved for AlN-based

Fig. 7 Electric field intensity enhancement factor (EFIEF) for different semiconductors

SPR sensor in comparison to GaN- and InN-based sensors. This happens due to the fact that the real part of complex refractive index of AlN is smaller than that of GaN and InN. Thus, from the above discussion, one can conclude that maximum EFIEF is achieved for semiconductors having smaller k -value and for smaller n value. From Fig. 7, it can be observed that electric FIEF of AlN is increased by a factor of 1.53, 2.45, 1.56 and 1.63 in comparison to the Si, Ge, GaN and InN, respectively.

Conclusion

In this work, a theoretical simulation is performed to observe the effect of semiconductor layer on sensitivity parameters and electric field enhancement factor of a graphene-based SPR biosensor. The effect of silicon, germanium and wurtzite III-V nitride materials on the sensitivity has been analysed. The simulation result shows that after placing the semiconductor in between active Ag metal and graphene, the sensitivity increases due to increase in $\Delta\theta$. For AlN, FWHM is 6.16° and the $\Delta\theta$ is increased by a factor of 4.17. This increase in $\Delta\theta$ is maximum, and FWHM is narrower in comparison to the other semiconductors. In addition, the electric field intensity is enhanced for the case of AlN by a factor of 1.53, 2.45, 1.56 and 1.63 with respect to Si, Ge, GaN and InN, respectively. This study suggests that for a high-performance graphene-based SPR biosensor, aluminium nitride (AlN) would be a better choice in comparison to other proposed semiconductor-based SPR biosensor. In addition, AlN layer can suppress the thermo-optic effects on sensitivity and it can be used for a variety of sensing applications including specific antibody detection, biological warfare agent detection and immune sensing.

Acknowledgments This work is supported by N.I.T Raipur under M.H.R.D Fellowship Scheme, Govt. of India.

References

- Nylander C, Liedberg CB, Lind T (1982) Gas detection by means of surface plasmons resonance. *Sensors Actuators* 3:79–88
- Liedberg B, Nylander C, Lundstrom I (1995) Biosensing with surface plasmon resonance—how it all started. *Biosens Bioelectron* 10:i–ix
- Homola J, Yee SS, Gauglitz G (1999) Surface plasmon resonance sensors: review. *Sensors Actuators B Chem* 54(1–2):3–15
- Homola J (2003) Present and future of surface plasmon resonance biosensors. *Anal Bioanal Chem* 377(3):528–539
- Van Regenmortel MH, Altschuh D, Chatellier J, Christensen L, Rauffer-Bruyere N, Richalet-Secordel P, Witz J, Zeder-Lutz G (1998) Measurement of antigen-antibody interactions with biosensors. *J Mol Recognit* 11:163–167
- Johansson B, Lofas S, Lindquist G (1991) Immobilization of proteins to a carboxymethyl-dextran-modified gold surface for biospecific interaction analysis in surface plasmon resonance sensors. *Anal Biochem* 198(2):268–277
- Thiel AJ, Frutos AG, Jordan CE, Corn RM, Smith LM (1997) In situ surface plasmon resonance imaging detection of DNA hybridization to oligonucleotide arrays on gold surfaces. *Anal Chem* 69(24):4948–4956
- Zalovsky Z, Abdulhalim I (2014) *Integrated nanophotonic devices*. Elsevier. pp. 221
- Jorgenson RC, Yee SS (1993) A fiber-optic chemical sensor based on surface plasmon resonance. *Sensors Actuators B Chem* 12:213–220
- Srivastava SK, Verma R, Gupta BD (2011) Surface plasmon resonance based fiber optic sensor for the detection of low water content in ethanol. *Sensors Actuators B Chem* 153:194–198
- Choi SH, Kim YL, Byun KM (2011) Graphene-on-silver substrates for sensitive surface plasmon resonance imaging biosensors. *Opt Express* 19(2):458–466
- Wu L, Chu HS, Koh WS, Li EP (2010) Highly sensitive graphene biosensors based on surface plasmon resonance. *Opt Express* 18(14):14395–14400
- Zhu XM, Lin PH, Ao P, Sorensen LB (2002) Surface treatments for surface plasmon resonance biosensors. *Sensors Actuators B Chem* 84(2–3):106–112
- Szunerits S, Maalouli N, Wijaya E, Vilcot JP, Boukherroub R (2013) Recent advances in the development of graphene-based surface plasmon resonance (SPR) interfaces. *Anal Bioanal Chem* 405(5):1435–1443
- Song B, Li D, Qi WP, Elstner M, Fan CH, Fang HP (2010) Graphene on Au(111): a highly conductive material with excellent adsorption properties for high-resolution bio/nanodetection and identification. *ChemPhysChem* 11(3):585–589
- Verma R, Gupta BD, Jha R (2011) Sensitivity enhancement of a surface plasmon resonance based biomolecules sensor using graphene and silicon layers. *Sensors Actuators B Chem* 160(1):623–631
- Kai-Qun KL, Lai-Ming W, Dou-Guo Z, Rong-Sheng Z, Pei W, Yong-Hua L, Hai M (2007) Temperature effects on prism-based surface plasmon resonance sensor. *Chin Phys Lett* 24(11):3081
- Jewett SA, Makowski MS, Andrews B, Manfra MJ, Ivanisevic A (2012) Gallium nitride is biocompatible and non-toxic before and after functionalization with peptides. *Actabiomaterialia* 8(2):728–733
- Maier SA (2007) *Plasmonics: fundamentals and applications*. Springer
- Raether H (1988) *Surface plasmons on smooth and rough surfaces and on gratings*. Springer, Berlin
- Hansen WN (1968) Electric fields produced by the propagation of plane coherent electromagnetic radiation in a stratified medium. *JOSA* 58(3):380–388
- Born M, Wolf E (1964) *Principles of optics: electromagnetic theory of propagation, interference and diffraction of light*. Pergamon Press, Oxford
- Zhan T, Shi X, Dai Y, Liu X, Zi J (2013) Transfer matrix method for optics in graphene layers. *J Phys Condens Matter* 25(21):215301
- Mohanty G, Sahoo BK, Akhtar J (2014) Comparative analysis for reflectivity of graphene based SPR biosensor. *Opt Quant Electron* 1–8
- SCHOTT optical glass data sheets 2012-12-04
- Johnson PB, Christy RW (1972) Optical constants of the noble metals. *Phys Rev B* 6:4370–4379
- Bruna M, Borini S (2009) Optical constants of graphene layers in the visible range. *Appl Phys Lett* 94:031901
- Aspnes DE, Studna AA (1983) Dielectric functions and optical parameters of Si, Ge, GaP, GaAs, GaSb, InP, InAs, and InSb from 1.5 to 6.0 eV. *Phys Rev B* 27:985–1009

29. Pastnák J, Roskocová L (1966) Refraction index measurements on AlN single crystals. *Phys Status Solidi* 14:K5–K8
30. Barker AS Jr, Ilegems M (1973) Infrared lattice vibrations and free-electron dispersion in GaN. *Phys Rev B* 7:743–750
31. Zubrilov A, Levinshtein ME, Rumyantsev SL, Shur MS (2001) Properties of advanced semiconductor materials GaN, AlN, InN, BN, SiC, SiGe. John Wiley & Sons, Inc., New York, pp 49–66
32. Hale GM, Querry MR (1973) Optical constants of water in the 200-nm to 200- μ m wavelength region. *Appl Opt* 12:555–563
33. Ong BH, Yuan X, Tjin SC (2006) Bimetallic silver-gold film waveguide surface plasmon resonance sensor. In *Integrated Optoelectronic Devices* (pp. 61230B–61230B). International Society for Optics and Photonics